Journal of the Korean Ceramic Society
Vol. 52, No. 6, pp. 462~466, 2015.

http://dx.doi.org/10.4191/kcers.2015.52.6.462

Transmission Electron Microscopy Investigation of Hot-pressed ZrB_2-SiC with B_4C Additive

Seongwon Kim†, Jung-Min Chae, Sung-Min Lee, Yoon-Suk Oh, Hyung-Tae Kim, and Byung-Koog Jang*

Engineering Ceramic Team, Korea Institute of Ceramic Engineering and Technology, Icheon 17303, Korea

**High Temperature Materials Unit, National Institute of Materials Science, Tsukuba, 305-0047, Japan*

(Received September 9, 2015; Revised October 15, 2015; Accepted October 16, 2015)

ABSTRACT

This paper reports the microstructure of hot-pressed ZrB_2-SiC ceramics with added B_4C as characterized by transmission electron microscopy. ZrB_2 has a melting point of 3245°C, a relatively low density of 6.1 g/cm^3, and specific mechanical properties at an elevated temperature, making it a candidate for application to environments with ultra-high temperatures which exceed 2000°C. Due to the non-sinterability of ZrB_2-based ceramics, research on sintering aids such as B_4C or $MoSi_2$ has become prominent recently. From TEM investigations, an amorphous layer with contaminant oxide is observed in the vicinity of B_4C grains remaining in hot-pressed ZrB_2-SiC ceramics with B_4C as an additive. The effect of a B_4C addition on the microstructure of this system is also discussed.

Key words : Ultra-high-temperature ceramics (UHTCs), ZrB_2-SiC, B_4C addition, Densification

1. Introduction

ZrB_2-based ceramics are among the most favorable candidates for ultra-high-temperature ceramics, including thermal protection systems (TPS) for leading edge parts on hypersonic planes, re-entry space vehicles, or propulsion systems as well as conventional applications such as furnace elements and refractory crucibles.[1-3] In order to accomplish these purposes, it is necessary to fabricate dense body parts made of ZrB_2-based ceramics. The densification of ZrB_2 powder generally requires very high temperatures due to the covalent nature of the bonds and due to the low bulk and grain boundary diffusion rates of ZrB_2.[4] Due to their non-sinterable characteristics, ZrB_2-based ceramics have been densified by a variety of methods, inducing hot pressing,[5-7] spark plasma sintering,[8-10] reactive hot pressing,[11,12] and pressureless sintering.[13-15]

Furthermore, sintering additives are frequently used in the ZrB_2-based system in order to enhance the densification in conjunction with various sintering techniques.[3,4] For example, two of the most commonly used sintering additives are $MoSi_2$[5,9] and B_4C,[6,13-15] which act as a liquid former or a reducing agent, respectively, enhancing the densification characteristics during sintering. On the other hand, oxygen impurities, such as B_2O_3 and ZrO_2, have been shown to promote grain coarsening by evaporation-condensation kinetics and to limit the final density in non-oxide ceramics.[16] In order to enhance the resulting density, it has been suggested that the total oxygen content must be reduced to less than 0.5 wt.% or that a strong reducing additive should be used to remove oxide contaminants. Given the current situation, B_4C is a reactive agent which enhances densification by reacting with and removing surface oxides on ZrB_2 particles. In our previous work,[6] it was reported that the hot pressing of ZrB_2-20 vol.% SiC at 1700°C for 2 h at a pressure of 30 MPa attained only a relative density of ~ 87%, whereas a relative density of ~ 95% was obtained for ZrB_2-20 vol.% SiC with an extra 5 vol.% of B_4C under identical hot pressing conditions.

Given that the mechanical properties of ZrB_2-based ceramics are closely related to the microstructure and the densification process and sintering additives used, a close examination of the microstructure is necessary to produce ZrB_2-based ceramics capable of enhanced performance levels. In this study, the microstructure of hot-pressed ZrB_2-SiC ceramics with B_4C as an additive was characterized by transmission electron microscopy. The grains and grain boundaries were analyzed using high-resolution imaging and energy dispersive X-ray spectroscopy (EDS) techniques. The effects of a B_4C addition on the densification and mechanical properties of ZrB_2-SiC are also discussed.

2. Experimental Procedure

ZrB_2-20 vol.% SiC and ZrB_2-20 vol.% SiC with an extra 5 vol.% of B_4C were prepared for this study using raw powders of ZrB_2 (Grade F; 1.88 μm, Japan New Metals. Co. Ltd.,

†Corresponding author : Seongwon Kim
E-mail : woods3@kicet.re.kr
Tel : +82-31-645-1452 Fax : +82-31-645-1492

Japan), α-SiC (FCP 15C; 0.5 μm, SIKA TECH, Germany), and B_4C (Grade A; 1.5 μm, UK Abrasives, USA). The samples were sintered by hot pressing. After weighing, the powders were mixed by planetary milling with WC-Co jars and balls in isopropyl alcohol for 4 h. The slurry of the powder mixture was vaporized by a hot plate upon stirring to create cakes, and the cakes of powder mixtures were dried in an oven for 24 h. The dried powder mixtures were then sieved with a #120-mesh sieve for granulation. The prepared powder mixtures were hot-pressed in a graphite mold. The hot pressing step was carried out at 1900°C for 2 h under a pressure of 30 MPa in a flowing Ar atmosphere.

For the hot-pressed samples, the densities, microstructures, and mechanical properties were characterized. The apparent densities were measured using the Archimedes method and the relative densities were calculated by comparing the apparent densities with the theoretical densities via the rule of mixture. The specimens were also ground with a diamond wheel and then polished from 6 to 1 mm of diamond slurry for a microstructure analysis and hardness measurements. The microstructures were examined using a field-emission scanning election microscope (FE-SEM, JSM-6701F, JEOL, Japan), and the Vickers hardness was measured by a micro-hardness tester (QM-2, Nikon, Japan).

Cross-sectional foils for the transmission electron microscopy analysis were sliced from the polished surface of the samples using a focused ion beam (FIB, Helios 600i, FEI, USA) with a Ga ion source accelerated at 30 kV. The slices were finally thinned with a fine ion beam current to less than 100 nm, which is an electron-transparent thickness in TEM. Thin foils of the samples were examined by a transmission electron microscope (TEM, Tecnai G2 F30, FEI, USA) equipped with an energy dispersive X-ray spectroscopy (EDS) analyzer.

3. Results and Discussion

In this study, the effects of an addition of B_4C on the microstructures of ZrB_2-SiC ceramics were determined using transmission electron microscopy.

Figure 1 shows the microstructure of the ZrB_2-20 vol.% SiC with or without 5 vol.% of added B_4C densified by hot pressing at 1900°C for 2 h. In the backscattered electron mode (BSE) of SEM, microstructural features with higher average atomic weights appear in brighter contrast. In Fig. 1, the gray matrix is ZrB_2, while the black dispersed particles denote the SiC. Table 1 summarizes the characteristics of the hot-pressed ZrB_2-based ceramics used in this study.

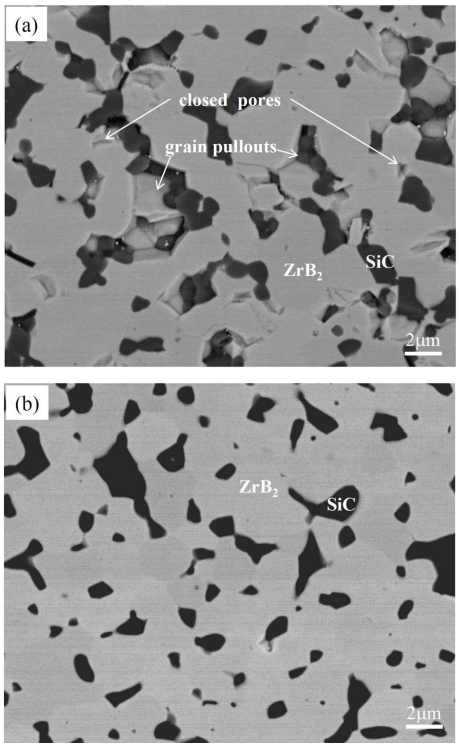

Fig. 1. SEM micrographs of ZrB_2-20 vol.% SiC with (a) no additives and (b) an extra 5 vol.% of B_4C hot-pressed at 1900°C for 2 h at 30 MPa.

Both samples exhibited almost full densities. While a considerable number of pores can be observed in Fig. 1(a), much of the apparent porosity is thought to be due to grain pullout during polishing, which resulted not from densification behavior but from the machining process.[14] Furthermore, the remaining B_4C is not discernible in this SEM micrograph.

Figure 2 shows typical bright-field TEM images of ZrB_2-20 vol.% SiC with an extra 5 vol.% of B_4C densified by hot pressing at 1900°C for 2 h. The microstructure was composed of three constituent phases, which were equiaxed ZrB_2 or SiC and elongated B_4C. Pores were rarely observed, except for those in the vicinity of B_4C particles. In the bright-field TEM images, diffraction contrast should be observed for the crystalline phases in the microstructure due to the periodicity of the atomic structure. In contrast, amorphous phases show lower contrast in bright-field images due to the absence of crystallite. In Fig. 2(b), an amorphous layer can be observed, especially near the B_4C particles.

Table 1. Composition, Sintering Condition, Density, and Vickers Hardness of Hot-pressed ZrB_2-based Ceramics Used in This Study

Compositions	Hot-pressing condition	Apparent density (g/cm^3)	Theoretical density (g/cm^3)	Relative density (% T.D.)	Vickers hardness (GPa)	
					R.T.	900°C
ZrB_2-20 vol.% SiC	1900°C/2 h/30 MPa /flowing Ar	5.47	5.51	99.3	19.7	8.5
ZrB_2-20 vol.%SiC with extra 5 vol.% B_4C		5.37	5.37	100	21.3	9.0

B_4C is one of the most frequently used sintering additives for the densification of ZrB_2-based ceramics.[13-15] The full densification of ZrB_2-based ceramics is known to be scarcely achievable due to the covalent nature of the bonding or the low diffusion rates.[3,4] Oxide layers on the surfaces of the starting powder have been shown to inhibit densification and to promote grain growth in boride ceramics systems.[16] The addition of B_4C to a ZrB_2-based system is known to enhance the densification by removing oxides during the heat treatment. These reactions proceed as follows[14]:

$$7ZrO_2 + 5B_4C \rightarrow 7ZrB_2 + 5CO(g) + 3B_2O_3(l) \quad (1)$$
$$2ZrO_2 + B_4C + 3C \rightarrow 2ZrB_2 + 4CO(g) \quad (2)$$
$$ZrO_2 + B_2O_3(l) + 5C \rightarrow ZrB_2 + 5CO(g) \quad (3)$$

In our previous work,[6] an addition of B_4C to a ZrB_2-SiC system enhanced the densification, especially at a relatively low temperature of 1700°C. On the other hand, the differences in the relative densities of ZrB_2-SiC ceramics hot-pressed at 1900°C for 2 h were not obvious, as shown in Table 1. In addition, ZrB_2-SiC ceramics with a B_4C addition hot-pressed at 1900°C for 2 h exhibited moderately higher density and hardness values.

In Fig. 3, the high-resolution TEM microstructures are shown to be present near the grain boundaries in hot-pressed ZrB_2-SiC with an addition of B_4C. In the HR images, crystalline phases, which are well aligned with the electron beam, show the lattice fringes. Each constituent phase, in this case ZrB_2, SiC, or B_4C, exhibited lattices fringes, of which the width was in agreement with the d-spacing of the relevant lattice plane, as denoted in Fig. 3. In particular, lattice fringes from SiC represented the ordered sequence of 6H-SiC, which corresponds to α-SiC. In addition, amorphous layers were observed especially near the B_4C grains in both images.

In order to identify the chemical composition of the amorphous layer, an energy dispersive X-ray spectroscopy analysis was carried out. Fig. 4 shows an STEM (scanning transmission electron microscopy) image and the EDS spectra obtained at the grain boundary as well as the constitu-

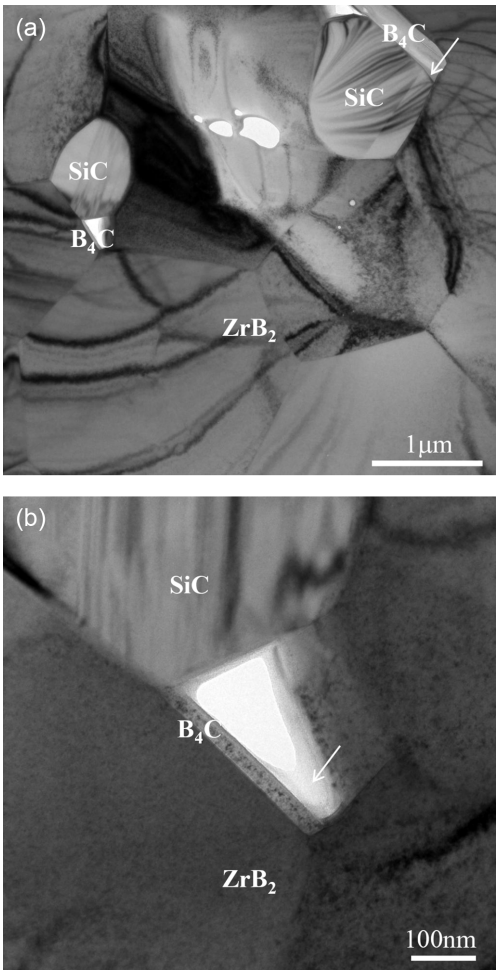

Fig. 2. (a) Bright-field transmission electron microscopy image and (b) a higher-magnification image of hot-pressed ZrB_2-20 vol.% SiC with an extra 5 vol.% of B_4C. (The arrow indicates the amorphous region near the B_4C grain.)

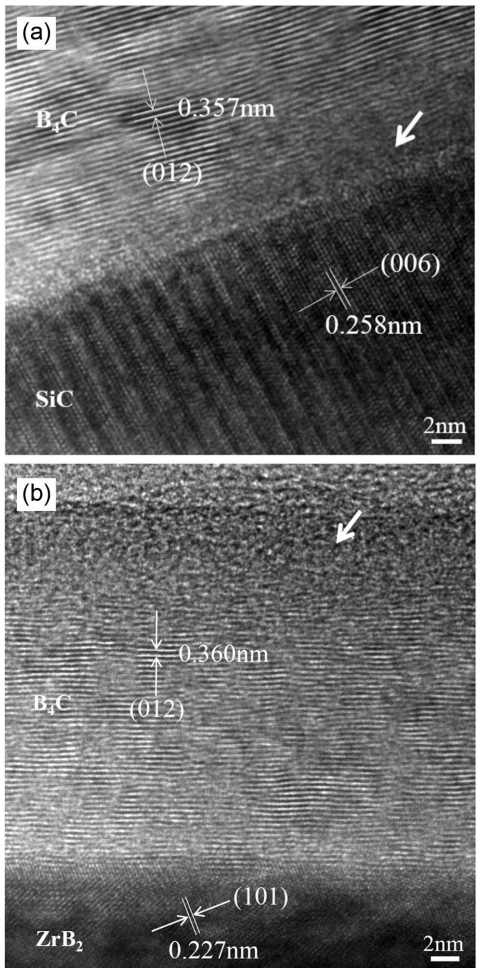

Fig. 3. High-resolution transmission electron microscopy images of grain boundaries in hot-pressed ZrB_2-20 vol.% SiC with an extra 5 vol.% of B_4C: (a) B_4C-SiC interface and (b) B_4C-ZrB_2 interfaces. (Arrows indicate the amorphous region near the B_4C grains.)

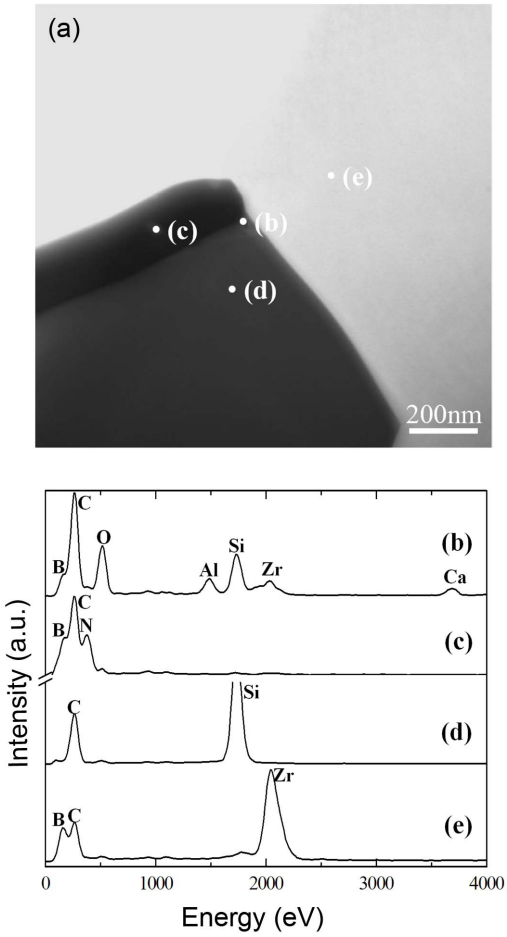

Fig. 4. (a) Scanning transmission electron microscopy image of hot-pressed ZrB_2-20 vol.% SiC with an extra 5 vol.% of B_4C and energy dispersive X-ray spectroscopy spectra from (b) the interface, (c) B_4C, (d) SiC, and (e) ZrB_2 as marked in (a).

ent phases. In the STEM images from a HAADF (high-angle annular dark field) detector, the elemental contrast could be seen similarly to the BSE mode in SEM.[17] In the microstructure, the elongated black particle corresponds to the B_4C. In the EDS spectra, it was noted that all spectra had carbon peaks due to carbon depositions during the STEM analysis. Fig. 4(b) presents the EDS spectra from the amorphous layer of a triple junction between ZrB_2, SiC, and B_4C. These spectra contained peaks from constituent elements such as Zr, Si, B, and C and from contaminants such as Ca, Al and O. It has been reported that oxide impurities are observable at the grain boundary and inside the grains of hot-pressed ZrB_2, while oxygen cannot be detected either inside the ZrB_2 grains or at the grain boundaries of the specimen densified by spark plasma sintering.[10] In this study, intergranular amorphous layers with oxide contaminants were observed exclusively in the vicinity of the B_4C grains. From these observations, B_4C was thought to absorb and react with oxide impurities as in the above-mentioned reactions of eq. (1) ~ (3) to enhance the densification of ZrB_2-based ceramics. On the other hand, oxide contaminants in ZrB_2-based ceramics can degrade the mechanical properties at an elevated temperature. A second-phase addition reduces the densification temperature and the grain size,[3] but the resulting ceramics may undergo degradation in their mechanical properties at an elevated temperature.[1] For example,[1] substantial differences were observed in the flexural behavior at temperatures which exceeded 1200°C among the materials with or without additives such as carbides, nitrides, and/or oxides. This type of strength degradation is claimed to be due to the softening of the glassy intergranular phases, which contribute to subcritical crack growth. Typically, oxide impurities form a grain boundary phase or become localized at triple junctions, which reduces the strength.[18]

4. Summary

The microstructure and the grain boundary phase of ZrB_2-SiC ceramics with added B_4C were examined by means of TEM. For hot-pressed ZrB_2-SiC ceramics with B_4C, the microstructure consisted of equiaxed ZrB_2 or SiC grains and a few elongated B_4C grains. Intergranular amorphous layers were observed especially near the B_4C grains. These amorphous layers exhibited EDS elemental peaks from constituent elements such as Zr, Si, B, and C and from contaminants such as Ca, Al and O.

Acknowledgments

This study was supported by a grant from the "Basic and Strategic R&D Program" funded by the Korea Institute of Ceramic Engineering and Technology, Republic of Korea.

REFERENCES

1. F. Monteverde, S. Guicciardi, and A. Bellosi, "Advances in Microstructure and Mechanical Properties of Zirconium Diboride Based Ceramics," *Mater. Sci. & Eng. A,* **346** [1-2] 310-19 (2003).
2. M. J. Gasch, D. T. Ellerby, and S. M. Johnson, "Ultra High Temperature Ceramic Composites," pp. 197-224 in Handbook of Ceramic Composite. Ed. by N. P. Bansal, Kluwer Academic Publishers, Boston/Dordrecht/London, 2005.
3. W. G. Fahrenholtz, G. E. Hilmas, I. G. Talmy, and J. A. Zaykoski, "Refractory Diborides of Zirconium and Hafnium," *J. Am. Ceram. Soc.,* **90** [5] 1347-64 (2007).
4. S. Q. Guo, "Densification of Zrb2-Based Composites and Their Mechanical and Physical Properties: A Review," *J. Eur. Ceram. Soc.,* **29** [6] 995-1011 (2009).
5. T. Mizuguchi, S. Q. Guo, and Y. Kagawa, "Transmission Electron Microscopy Characterization of Hot-Pressed ZrB_2 with $MoSi_2$ Additive," *J. Am. Ceram. Soc.,* **92** [5] 1145-48 (2009).
6. J.-M. Chae, S.-M. Lee, Y.-S. Oh, H.-T. Kim, K.-J. Kim, S. Nahm, and S. Kim, "Effect of B_4C Addition on the Microstructures and Mechanical Properties of ZrB_2- SiC Ceram-

ics (*in Korean*)," *J. Korean Ceram. Soc.,* **47** [6] 578-82 (2010).
7. D. D. Jayaseelan, Y. Wang, G. E. Hilmas, W. Fahrenholtz, P. Brown, and W. E. Lee, "TEM Investigation of Hot Pressed-10 Vol.% SiC-ZrB_2 Composite," *Adv. in Appl. Ceram.,* **110** [1] 1-7 (2011).
8. V. Medri, F. Monteverde, A. Balbo, and A. Bellosi, "Comparison of ZrB_2-ZrC-SiC Composites Fabricated by Spark Plasma Sintering and Hot-Pressing," *Adv. Eng. Mater.,* **7** [3] 159-63 (2005).
9. A. Bellosi, F. D. Monteverde, and D. Sciti, "Fast Densification of Ultra-High-Temperature Ceramics by Spark Plasma Sintering," *Int. J. Appl. Ceram. Technol.,* **3** [1] 32-40 (2006).
10. T. Mizuguchi, S. Q. Guo, and Y. Kagawa, "Transmission Electron Microscopy Characterization of Spark Plasma Sintered ZrB_2 Ceramic," *Ceram. Int.,* **36** [3] 943-46 (2010).
11. G. J. Zhang, Z. Y. Deng, N. Kondo, J. F. Yang, and T. Ohji, "Reactive Hot Pressing of ZrB_2- SiC Composites," *J. Am. Ceram. Soc.,* **83** [9] 2330-32 (2000).
12. J. W. Zimmermann, G. E. Hilmas, W. G. Fahrenholtz, F. Monteverde, and A. Bellosi, "Fabrication and Properties of Reactively Hot Pressed ZrB_2- SiC Ceramics," *J. Eur. Ceram. Soc.,* **27** [7] 2729-36 (2007).
13. S. C. Zhang, G. E. Hilmas, and W. G. Fahrenholtz, "Pressureless Densification of Zirconium Diboride with Boron Carbide Additions," *J. Am. Ceram. Soc.,* **89** [5] 1544-50 (2006).
14. S. Zhu, W. G. Fahrenholtz, G. E. Hilmas, and S. C. Zhang, "Pressureless Sintering of Zirconium Diboride Using Boron Carbide and Carbon Additions," *J. Am. Ceram. Soc.,* **90** [11] 3660-63 (2007).
15. S. C. Zhang, G. E. Hilmas, and W. G. Fahrenholtz, "Pressureless Sintering of ZrB_2-SiC Ceramics," *J. Am. Ceram. Soc.,* **91** [1] 26-32 (2008).
16. S. Baik and P. F. Becher, "Effect of Oxygen Contamination on Densification of TiB_2," *J. Am. Ceram. Soc.,* **70** [8] 527-30 (1987).
17. L. C. Feldman and J. W. Mayer, "Fundamentals of Surface and Thin Film Analysis," Elsevier Science Publishing Co. Inc., New York, 1986.
18. F. Monteverde and A. Bellosi, "Efficacy of HfN as Sintering Aid in the Manufacture of Ultrahigh-Temperature Metal Diborides-Matrix Ceramics," *J. Mater. Res.,* **19** [12] 3576-85 (2004).